IEEE Access
Multidisciplinary | Rapid Review | Open Access Journal

Received May 1, 2022, accepted May 16, 2022, date of publication May 23, 2022, date of current version June 2, 2022.

Digital Object Identifier 10.1109/ACCESS.2022.3177660

Energy Optimization of Air Handling Units Using Constrained Predictive Controllers Based on Dynamic Neural Networks

OMID ASVADI-KERMANI[1], (Graduate Student Member, IEEE), HAMIDREZA MOMENI[1], (Senior Member, IEEE), ANDREA JUSTO[2], JOSEP M. GUERRERO[3], (Fellow, IEEE), JUAN C. VASQUEZ[3], (Senior Member, IEEE), JOSE RODRIGUEZ[4], (Life Fellow, IEEE), AND BASEEM KHAN[5], (Senior Member, IEEE)

[1]Department of Control, Faculty of Electrical and Computer Engineering, Tarbiat Modares University, Tehran 14117-13116, Iran
[2]Department of Psychobiology and Methodology of Health Sciences, Universitat Autònoma de Barcelona, 08193 Bellaterra, Spain
[3]Center for Research on Microgrids (CROM), AAU Energy, Aalborg University, 9220 Aalborg, Denmark
[4]Faculty of Engineering, Universidad San Sebastian, Santiago 8420524, Chile
[5]Department of Electrical and Computer Engineering, Hawassa University, Hawassa 05, Ethiopia

Corresponding author: Baseem Khan (baseem.khan04@gmail.com)

This work was supported by the VILLUM FONDEN through the VILLUM Investigator Grant: Center for Research on Microgrids (CROM) (www.crom.et.aau.dk) under Grant 25920. The work of Jose Rodriguez supported by ANID under Project FB0008 and Project 1210208.

ABSTRACT Optimizing energy consumption in buildings is a significant challenge in today's society. A major part of energy consumption is in heating, ventilation and air conditioning (HVAC) systems. In this paper, the aim is to reduce the energy consumption of air handling units (AHU) by applying optimal control. This system used in this study has four AHUs, all of which are assumed to be the same. Due to the uncertainty of the temperature of the heat exchanger's (H/E) inlet and outlet water, a model of the system was first made using its hypothetical capacity according to the ASHRAE standards. The inlet and outlet water temperatures are calculated using simulated and real data. In order to increase the model's accuracy and facilitate implementation on a real system, the data obtained is used to train a dynamic recurrent neural network (RNN) for the H/E. Furthermore, to increase the system's stability and bolster its response to disturbances, which change system parameters over time and reduce the accuracy of neural network models, an online recursive least squares (RLS-based) adaptive constrained generalized predictive controller (AGPC) is used to control its outlet air temperature. The AGPC attempts to minimize the computational load and estimates the transfer function by using continuously updated input-output data from the model; this model has fewer parameters than the RNN model. Finally, the power consumption of the H/E is calculated. The outlet humidity and airflow are controlled using an optimal controller to minimize energy consumption. The results show a reduction in the energy consumption of 54.95% with respect to the previous work and of 69.9% compared to the dataset from the real system.

INDEX TERMS Predictive controller, adaptive control, air handling unit, energy optimization, dynamic neural networks.

NOMENCLATURE

Symbol	Definition	Value
$\mathbf{T_{sa,i}}$	Air temperature in the outlet of AHU_i in °C	
$\mathbf{T_{sai,ref}}$	Air temperature reference in the outlet of AHU_i in °C (Supply air temperature in zones)	
$\mathbf{T_{Ri}}$	Recirculation air temperature of AHU_i in °C	
$\mathbf{T_o}$	External air temperature in °C	
$\mathbf{H_o}$	Outside air relative humidity percentage	
$\mathbf{P}$	Prediction horizon	5
$\mathbf{M}$	Control horizon	5
$\mathbf{T_s}$	Sampling time (s)	300
$\mathbf{G_{a,i}}$	Airflow rate in the outlet of AHU_i in $(kg)s^{-1}$	

The associate editor coordinating the review of this manuscript and approving it for publication was Shihong Ding.

$\mathbf{G_{ri}}$	Recirculation airflow rate of AHU_i in $(kg)s^{-1}$	
$\mathbf{G_o}$	Outside airflow rate of AHU units in $(kg)s^{-1}$	
$\mathbf{G_w}$	Water flow rate in H/E of AHU units in $(kg)s^{-1}$	1
$\mathbf{OA_i}$	Recirculation air amount of damper opening of AHU_i	
$\mathbf{H_{outi}}$	Air relative humidity percentage in the outlet of AHU_i	
$\mathbf{a_{ga}}$	Heat transfer coefficient on the air-side in the H/E of AHU units $(kW)(m^2.°C)^{-1}$	0.025
$\mathbf{a_{gw}}$	Heat transfer coefficient on the water side in the H/E of AHU units $(kW)(m^2.°C)^{-1}$	0.013
$\mathbf{c_g}$	Mass specific heat of H/E shell wall in AHU units $(kJ)(kg.°C)^{-1}$	0.89
$\mathbf{M_g}$	Mass specific heat of H/E shell wall inAHU units (kg)	5.13
$\mathbf{l}$	Length of coiled tube in H/E of AHU units (m)	114.0
$\mathbf{A_0}$	Air-side surface of heat exchanger of AHU units $(m)^2$	6.58
$\mathbf{A_i}$	Water-side surface of AHU's H/E units $(m)^2$	0.782
$\mathbf{A_w}$	Cross section area of coiled tube in AHU's H/E units $(m)^2$	$3.4*(10)^{-5}$
$\boldsymbol{\eta_s}$	Efficiency of sensible heat exchange of AHU units	0.75
$\mathbf{T_{g,i}}$	Temperature of heat shell wall of H/E in $AHU_i(°C)^{+1}$	
$\mathbf{T_{m,i}}$	Average surface temperature of fins in H/E of $AHU_i°C$	
$\mathbf{T_{outi,w}}$	Outlet water temperature in H/E of $AHU_i°C$	
$\mathbf{T_{ini,w}}$	Inlet water temperature in H/E of $AHU_i°C$	
$\boldsymbol{\rho_w}$	Water density $(kg)(m^3)^{-1}$	1000
$\mathbf{c_w}$	Water mass specific heat $(kJ)(kg.°C)^{-1}$	4.186

I. INTRODUCTION

Increasing energy consumption is one of society's main concerns today. A large portion of overall energy usage takes place in buildings (about 30 %) [1], and a significant part of this energy is related to ventilation, cooling, and heating systems (about 50%) [2]. Maintaining the temperature and humidity of the ambient air within the standard range to create thermal comfort is one of the important points that should be considered in the design of a ventilation system. In this paper, the aim is to maintain these parameters within the desired range for thermal comfort while reducing the HVAC system's energy consumption.

This paper builds on many existing studies in the field. Reference [3] investigated the dataset from a four-AHU ventilation system in a medium-large size building located in Romania [4], [5]. Romania is a four-season country with hot summers and cold winters, and optimizing cooling and heating systems in this context is particularly important. The data had been collected over a period of one year. The ventilation space model of the system was estimated using series neural networks, and the model predictive controller (MPC) was distributed on the system. The energy efficiency of the system, in general, was specified.

Reference [6] implemented an MPC on an HVAC system and then estimated it using recurrent neural networks. That paper investigated energy consumption over a period of just one month in different seasons, and its scope was limited to the cooling system. Reference [7] used a feedforward neural network (FFNN), a radial basis function network (RBFN), and an adaptive neuro fuzzy inference system (ANFIS) to predict the energy consumption of a heating system. Results were investigated over a period of 1.5 months. In all of these references, the main goal is to predict the energy consumption of the system using these neural networks directly that need a lot of data from the system. But, this research's main goal is reducing the total energy consumption of the system in the online form, using an adaptive neural-based predictive controller and constrained optimal controller. Due to the dynamic nature of the heat exchanger system, dynamic and recurrent neural networks (RNN) only have been used for modeling the system s' heat exchanger with good accuracy. Reference [8] discussed different kinds of artificial neural network (ANN)-based MPCs. Reference [9] investigated the computational load problem of MPC controllers. References [10], [11] reduced the computational load of an MPC controller by using linear models to simplify the building model. Reference [12] incorporated MPC into the state-space model of an office building. Reference [13] achieved an energy-saving percentage of about 27.01%, which was calculated over a 24-hour period.

This work, in contrast, calculates the energy-saving percentage over a period of one year and investigates the energy consumption in different parts of the AHU units. The model of each component of the HVAC system has been specified in detail. Some equations, like energy consumption and nonlinear equations, which have been used for modeling components, are quite complex. It should be noted that achieving a good performance can be more challenging when longer time periods are used. This paper uses a variable air volume AHU. The ANN feed-forward neural network approach with 20 layers has been used as a secondary method to specify the setpoint.

Ref. [14] used a system state-space model of the whole HVAC system and the zones it supplied. The model is complex, and it has nonlinear states that increase the system's complexity. That study investigated the AHU and building structure. In addition, the authors implemented the controller in the centralized configuration system. In this work, on the

other hand, an adaptive constrained GPC controller has been implemented on a simplified estimated model to reduce the computational load. Three types of controllers: integrated fuzzy PI-PD Mamdani, cluster adaptive training based on Takagi Sugeno-Kang (CABTSK), and bang-bang have been applied to the system. Tuning these controllers can be challenging when the system parameters are in flux. The setpoint span of the indoor temperature has been specified according to the ISO7730 standard. In (ref), the energy consumption was investigated over a period of just 24 hours, whereas this work uses a period of one year; the energy efficiency of (ref) is about 37%; this study, meanwhile, has achieved a reduction of 54%.

Numerous other techniques have been proposed for energy optimization; however, many of them are complex and increase the computational load. Reference [15] investigated optimization problem solver tools for MPC controllers. Reference [16] specified MPC's limitations that stand in the way of its wider adoption in building control systems. Transfer learning with feed-forward deep neural networks for MPC has been presented in [17]. A predictive adaptive controller has been presented in [18]. A purely data-driven black-box model employing various choices of machine learning approaches has been illustrated in [19]. A comprehensive report of MPC controller benefits can be found in [20]. An RC model has been used to estimate the building model and simplify it in [21]. Reference [22] utilized simulated data from an MPC-controlled HVAC system and the adaptive boosting method to define decision rules. Distributed classic adaptive controllers that are implemented on the white box model have been illustrated in [23].

Reference [24] implemented an MPC strategy with encoder-decoder recurrent neural networks for the smart control of a thermal environment and achieved a 7% increase in energy efficiency. The method was implemented by considering the interaction between some of the system variables, and the result was compared with those of a PI controller and an adaptive PI controller. However, the complexity of the method, the high volume of calculations, the short duration of the experiment (about 4 hours) and the low improvements in energy efficiency (between 4 and 7%) are disadvantages of said work. Furthermore, [24] only addressed the control of the AHU's outlet air temperature.

Reference [25] studied the energy efficiency of five structures of the air conditioning system; the study improved the energy consumption of the cooling system by adding air-to-air H/E to the structure of each AHU. Energy demand fell by 23.68%, improving the efficiency of the first law by 31.29%. Similarly, the total energy losses were reduced by 26.58%, and the second law's efficiency was improved by 11.79%. A cost analysis showed that the lowest payback time and the highest cost savings were related to the first and fourth structures, respectively and this study in took place over a one-year period. A drawback of [25], however, is that it only investigates the modeling section, and it does not provide information about the performance of different control techniques for layouts with five AHUs.

Reference [26] achieved an energy consumption reduction of about 10% in a cooling system with variable air volume (VAV) AHUs using the ANN model and a developed controller. Reference [27] used data mining techniques to reduce the energy required by an HVAC system energy by about 23%. Two energy-based control techniques have been investigated in [28], and the energy usage was reduced by about 13%. Reference [29] developed a dynamic model for an HVAC system using schedule-based temperature and a damper position rest to reduce annual energy consumption. Reference [30] used a heat recovery method to reduce energy consumption in buildings. Ref [31] is about the FPGA-based Taguchi-chaos-particle swarm optimization (PSO) sun tracking system. In this reference, PI controller has been considered as the main controller. PSO algorithm has been used to tune PI controller parameters. Taguchi Method and Logistic Map have been used to increase steady-state convergence of PSO algorithm. The main goal is Maximum PowerPoint Tracking of the solar panel to increase its output power. PI is an unconstrained simple classical controller with a small degree of freedom. Because of its basis in online form implementation, PSO algorithm can increase the computational burden of the system and decrease speed of the controller. Also, the closed-loop system guarantee always is a challenge. Results just have been investigated in the small duration. In this work, an adaptive constrained predictive controller with consideration to computational burden reduction and better closed-loop stability has been developed. Ref [32] is about the solar-powered Stirling engine analysis and optimization with heat transfer considerations. The genetic algorithm has been used to compute the engine's maximum output power and its associated system characteristics. Exact physical model of the system has been used that it can change over the time and all parameters in real system have uncertainties. There are no details about optimization cost function and its constrains and considered genetic algorithm.

Because the actual structure of air conditioners in the real system is not known, this paper considers a common structure for all air conditioners that is detailed in [33]. Their capacity has been assumed the same to facilitate the system analysis. The capacity of the AHUs is considered the same as that of the AHU used in [3] (i.e. 1000 CFM) to facilitate the comparison of their energy consumption. In this work, the control system is divided into two parts: control of the outlet air temperature and control of the flow and humidity of each AHU's exhaust air. In the outlet air temperature control, since the temperatures of the inlet and outlet water of the H/E are unknown, these variables are first estimated using the proposed dynamic model with parameters from a real water to air H/E of the same capacity. In order to increase the accuracy and flexibility of the model, a dynamic linear neural network is used to estimate the overall model of the H/E. One of the innovations of this paper is that it combines data-based and model-based methods to increase accuracy. Real system data

and simulation data are used to estimate the H/E model. The adaptive constrained generalized predictive controller is used to increase the system's stability and ensure an appropriate response to disturbances and possible changes in the system. Another unique contribution of this article is that it considers the computational load in the design of the controller and attempts to reduce it. The humidity and airflow of each AHU are kept within the desired range by using a controller that seeks to optimize the system's energy consumption (Fig. 1). In this paper, MATLAB software is used for simulation.

Main advantages summerize of this work that have specified according to the research gaps that have been investigated previously, are described as follows in the end of this section:

a) Using a one-year dataset from a four-season country with hot summers and cold winters. The simulation also represents a year-long period.
b) Utilizing both physical and RNN-based data-driven models of the H/E. A physical model has been used to
c) estimate the unknown data of the H/E and HVAC system and to increase the accuracy of the main dynamic neural
d) network model that is estimated for the H/E. In addition, the main RNN model increases the flexibility of the proposed model such that it can be implemented in real system applications; it also ensures that the simulation results are as close to the actual system results as possible.
e) Attempting to control all essential HVAC parameters, including AHU outlet airflow rate, temperature, and humidity, and keep them within the standard range while optimizing energy consumption.
f) Using dynamic models only for the H/E and AHU outlet air temperature section so as to simplify the model and reduce the computational load. A non-dynamic model is used to control the AHU outlet air humidity and airflow.
g) Using online recursive least squares (RLS-based) adaptive constrained generalized predictive control (GPC) to control the system's outlet air temperature and in turn increase the stability of the system. This improves the system's response to disturbances, such as parameters that change over time, which reduce the accuracy of neural network models. The reduction of the computational load is also considered; to that end, the system's transfer function is estimated using continuously updated input-output data
from the model, and it thus has fewer parameters than the RNN model.
h) The results show a reduction in the energy consumption of 54.95% with respect to the previous work and of 69.9% compared to the dataset from the real system.

This study has five sections. Section II reviews water to air H/E modeling. Section III examines AHU output temperature, airflow, and humidity control. In section IV, the controllers' simulation results have been investigated in detail. Section V provides the conclusion of the paper.

II. WATER TO AIR HEAT EXCHANGER MODELING

As described in [3], the distributed MPC algorithm is implemented on the system state-space model, which is estimated using dynamic neural networks. According to Nomenclature and the reference signal assigned to the air temperature of the ventilated areas, the appropriate value of the outlet air temperature of each AHU $T_{sai,ref}$ has been calculated to reach the reference signal. In this article, the aim is to optimize the energy consumption of the air conditioners. Therefore, the inlet water temperature is considered as a control variable. Due to the uncertainty of the value of the inlet and outlet water temperature ($T_{ini,w}$, $T_{outi,w}$), it is assumed that the capacity of the AHU units is the same of those used in [3], and an estimate of these values is made using the general model intended for H/Es in [33] along with information about the parameters of the water to air H/Es laid out in the ASHRAE standards [34], [35]. To simplify the model, it has been assumed in Nomenclature that the H/E input and outlet air humidity are equal. The equations for the dynamic model equations are as follows:

$$\begin{cases} T_{i,w} = \frac{T_{ini,w}+T_{outi,w}}{2}, & T_{i,d} = T_{ini,w} - T_{outi,w} \\ T_{m,i} \simeq 0.96\, T_{sai,ref}, & \frac{dx}{d\tau} \simeq \frac{x(t) - x(t-1)}{T_s} \end{cases}, \quad (1)$$

$$\underbrace{\rho_w c_w A_w l \frac{dT_{i,w}}{d\tau} = G_w c_w T_{i,d} + a_{gw} A_i \left(T_g - T_{i,w}\right)}_{\text{Mass and energy equation of H/E coils}}, \quad (2)$$

$$T_{m,i} = \eta_s T_{g,i} - (1 - \eta_s)\, T_{i,w}. \quad (4)$$

This HVAC system has four AHUs that have been divided into two pairs ($AHU_{1,2}$& $AHU_{3,5)}$ [3]. More details are provided in in Fig. 2.

As per the instructions of [33], a common structure has been specified for each AHU in equations (2,3,17); this structure is depicted in Fig. 3. After calculating the inlet and outlet water temperature of the H/E for two AHU units, the main model of the H/E is estimated using linear autoregressive neural networks. The reason for using this data-driven approach for system modeling is that this method has enough flexibility to model complex systems with sufficient accuracy. In addition, this method can be implemented on real systems. It is possible to estimate this model using real control system data instead of dynamic model data. In this paper, two-layer linear time-series dynamic neural networks have been used to estimate the AHU units' outlet water temperature $T_{out,i}$ and their outlet air temperature $T_{sa,i}$ in the models of each AHU. These neural networks have been estimated using the MATLAB nonlinear autoregressive with external input (NARX) neural networks toolbox [36], [37]. To that end, 70% of data has been used to train the model, 15% has been used for validation, and the remaining 15% of data has been used to test the neural networks. The training function is the Levemberg-Marquardt

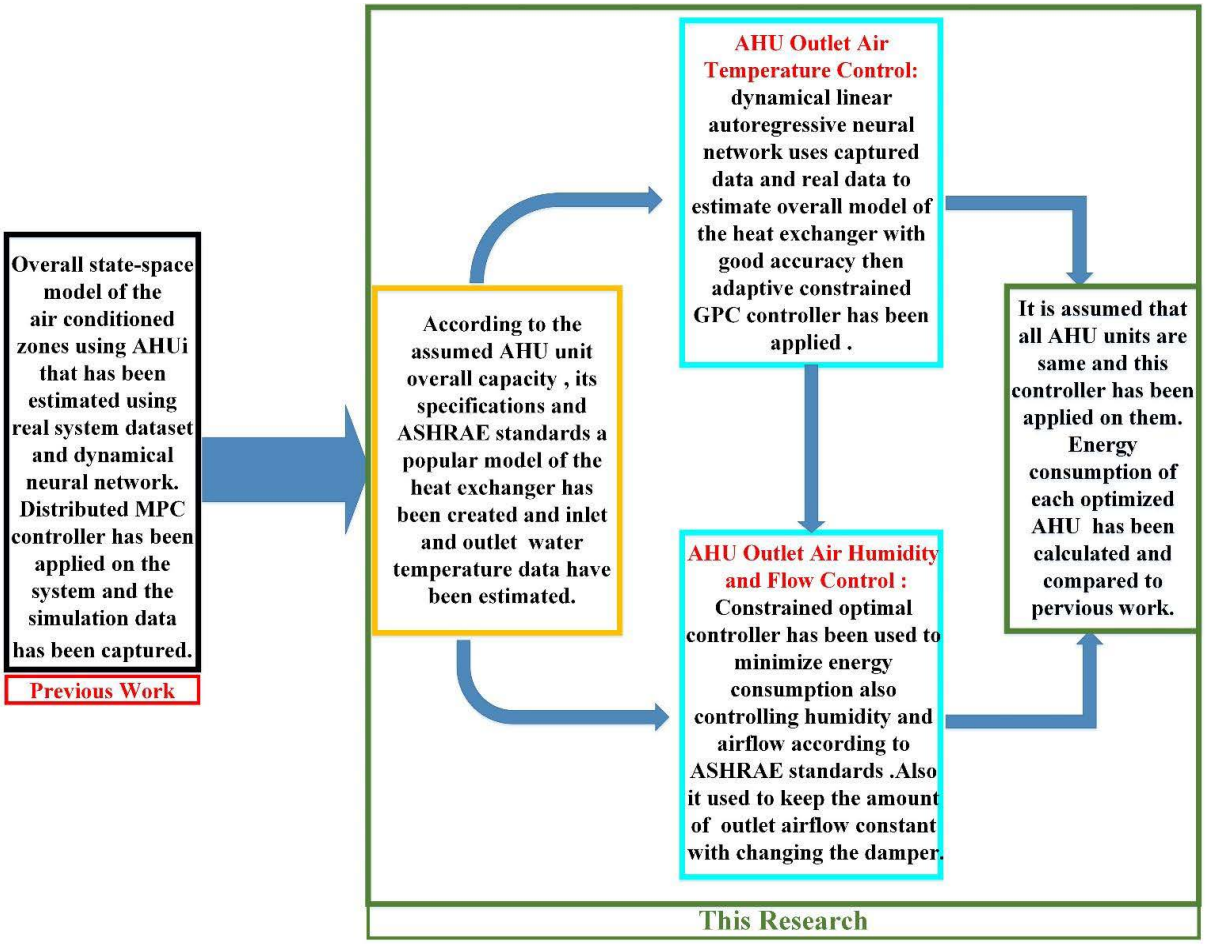

FIGURE 1. Methodology scheme (main parts of the work in overall form).

[38] algorithm, and the performance cost function is the mean square error (mse). The overall form of these neural networks is shown in Fig. 4.

The dataset from [4] (T_o, H_o), simulation data from [3] ($T_{sai,ref}$, T_{ri}), and the estimated data described in the first part of section 2 ($T_{ini,w}$, $T_{out,i}$) were used to train, validate, and test the neural networks.

A. REAL SYSTEM DATASET DESCRIPTION

Dataset [3], [4] related to 4 air handling units in a medium-large sized building (PRECIS research center) in Romania has been used. In temperate continental weather with hot summers and cold winters. On-site electric chillers offer cooling, while a district heating network provides warmth. Sensors individually measure the temperature data with each AHU. AHU 1 and AHU 2 are located on the roof of the building and are in charge of ventilation on floors 4-7, which are mostly research labs. While AHU 3 and AHU 5 are responsible for the building's lower levels, including administrative, multifunction, and technical facilities. Exhaust, intake, and recirculation air temperatures are all monitored by sensors in each AHU. The data is gathered at five-minute intervals and covers the entire year of 2017.

B. SIMULATION DATASET DESCRIPTION

In [3], simulation results of 4 AHU units have been specified for one year duraiton. These simulations have been done in the outside environment condition that has been specified in [4]. AHU units outlet air temperature ($T_{sa,ref}$) and recirculation air temperature (T_{ri}) data have been used in the modeling and control section of this paper.

$$\underbrace{M_g c_g \frac{dT_{g,i}}{d\tau} = a_{gw} A_i \left(T_{i,w} - T_g\right) + a_{ga} A_o \left(\frac{T_{sai,ref} + T_{ri}}{2} - T_{m,i}\right)}_{\text{Energy equation}}, \tag{3}$$

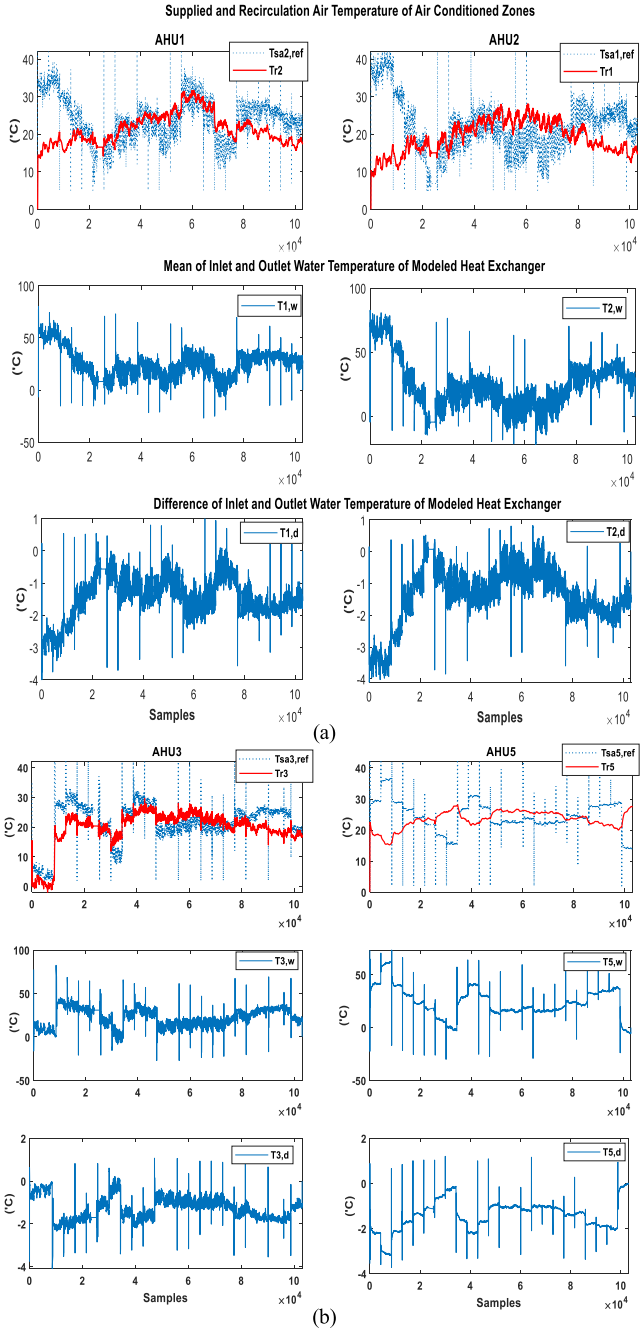

FIGURE 2. **(a) (b) H/E inlet and outlet water temperatures estimated using the model created for $AHU_{(1,2)}$ & $AHU_{(3,5)}$ (equations 2&3).**

The results (Figs. 5 and 6) show that there is a complete linear relation between the output and target data and that R is a regression factor equal to 1. The accuracy of the estimated model is perfect, and the data fit the estimated model completely.

(K_{wi}, K_l, h_l, h_{wi}, W_{wi}, W_l, b_l, b_{wi}, W_r) are weight matrices of these neural networks. Each layer has the Purelin transfer function.

According to neural network model flexibility, the main goal of this section is to estimate a generalized data-driven model for each AHU heat exchanger with good accuracy.

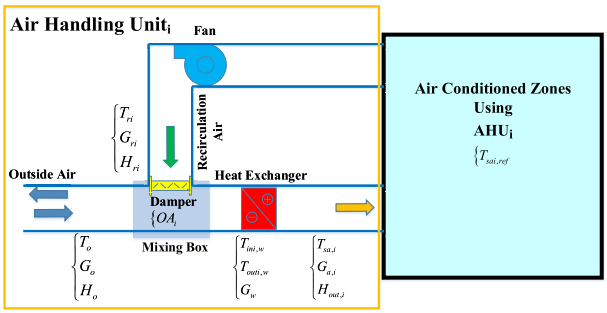

FIGURE 3. **Overall structure that has been used for the AHUs in this paper.**

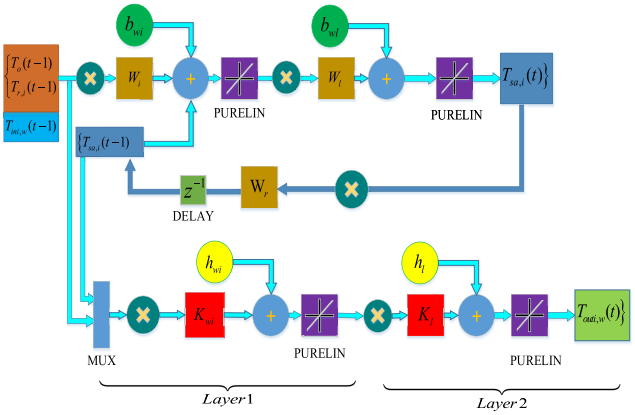

FIGURE 4. **Overall structure of H/E linear dynamic time-series neural network model for AHU_i.**

Due to figure 4 overall model has 2 parts. First part is that the main dynamic recurrent neural network model has been estimated to model outlet air temperature (T_{sa}). Figure 5 shows that the R = 1 and gradient and estimation error are very small approximately is zero. It is reason most of the data that has been used for estimation of the model captured from linear system simulation in [3] and the first part of section II estimated model output completely fit on the dataset. The neural network layers and neurons have been considered as small as possible to avoid its overfitting. Second part of the model is a feed-forward neural network model of the H/E outlet water temperature. This model has been considered to complete the overall model. Also, in analyzing its results has helped to increase accuracy and close estimated model to real system application. In two parts neural networks has 2 layers and 2 neurons in each node.

III. AHU OUTPUT TEMPERATURE, AIRFLOW, HUMIDITY CONTROL

A. AHU OUTLET AIR TEMPERATURE CONTROL

In the previous section, the H/E model was estimated using neural networks. Because the data used to train the neural network is collected from a closed-loop controlled system, this neural network can act as a controller to regulate the output temperature $T_{sa,i}$ of the AHU. The disadvantage of this method is that if the values of the reference signal and input signals change or the system parameters change, the output of the system may be suboptimal. Another disadvantage is that if the neural network model is estimated online, the large

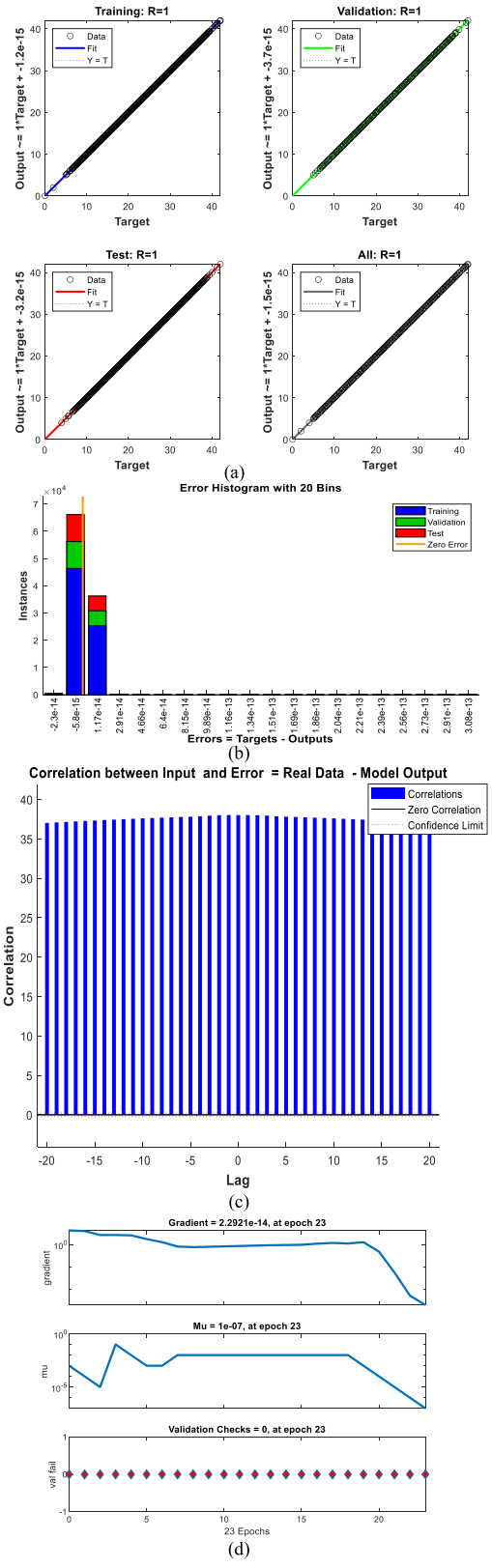

FIGURE 5. (a) (b) (c) (d) AHU1 outlet air temperature $T_{sa,i}$ dynamic neural network model estimation results.

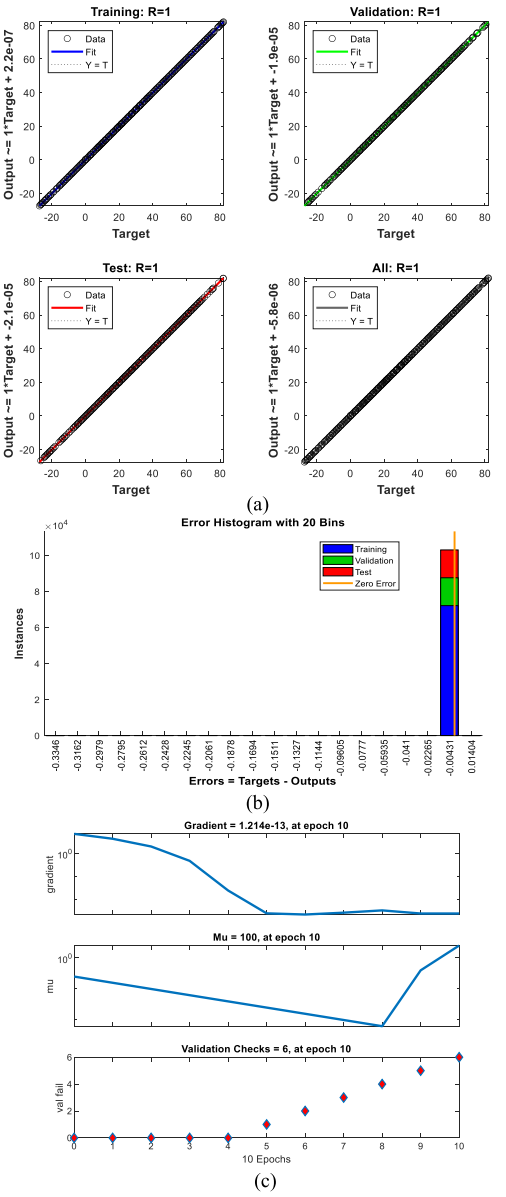

FIGURE 6. (a) (b) (c) AHU1 outlet water temperature $T_{outi,w}$ neural network model estimation results.

number of parameters causes this model to put a significant computational burden on the controller hardware, and the system therefore requires more powerful hardware for its implementation. The proposed solution is to use an auxiliary adaptive controller to increase system stability and maintain output convergence in the presence of disturbances. MPC is one of the optimization-based control methods that is used in many systems due to its desirable features such as enhanced system stability and its ability to neutralize the effect of disturbances; another advantage is that it can be implemented despite constraints. The disadvantages of this controller are its complexity and the large volume of its calculations [39], [40].

Due to the large number of parameters in the neural network model, the computational burden will be high if the controller is applied to it. In order to reduce said burden, this study uses a different MPC method called generalized

predictive control (GPC). In this method, only the input-to-output transfer function of the system is used to implement the controller. One benefit of this method is that it can be implemented on non-minimum phase

systems and even unstable systems. It also responds well to disturbances. The GPC controller equations are specified below:

$$A\left(z^{-1}\right) = 1 + a_1 z^{-1} + \ldots. + a_{n_a} z^{-n_a},$$
$$B\left(z^{-1}\right) = b_0 + b_1 z^{-1} + \ldots. + b_{n_b} z^{-n_b},$$
$$C\left(z^{-1}\right) = c_0 + c_1 z^{-1} + \ldots. + c_{n_c} z^{-n_c},$$
$$\Delta\left(z^{-1}\right) = 1 - z^{-1},$$
$$\textbf{\textit{CARIMA Model}}: A\left(z^{-1}\right) y\left(t\right) = z^{-d} B\left(z^{-1}\right) u\left(t-1\right) + \frac{C\left(z^{-1}\right) e\left(t\right)}{\Delta\left(z^{-1}\right)}, \quad (5)$$

where the polynomial $A(z^{-1})$ is the model output dynamic and the polynomials $B\left(z^{-1}\right)$ and $C(z^{-1})$ are the control input and disturbance dynamics, respectively. n_a, n_b, and n_c are the degrees of these polynomials. d is the input delay. $\Delta\left(z^{-1}\right)$ is an integrator that has been added to the model to prevent steady-state error. The desired control signal $u(t)$ is generated by minimizing the cost function (J_c). This cost function is optimized iteratively in every sequence of the control algorithm. The prediction output is calculated over the prediction horizon using the Diophantine equation in which $C\left(z^{-1}\right)$ is white Gaussian noise. (In this paper $C\left(z^{-1}\right) = 0, d = 0.$):

$$\tilde{A}\left(z^{-1}\right) = \Delta A\left(z^{-1}\right) \to 1 = E_j\left(z^{-1}\right)\tilde{A}\left(z^{-1}\right) + z^{-j} F_j\left(z^{-1}\right), \quad (6)$$
$$E_j\left(z^{-1}\right) = e_{j,0} + e_{j,1} z^{-1} + \ldots. + e_{j,j-1} z^{-(j-1)}, \quad (7)$$
$$F_j\left(z^{-1}\right) = f_{j,0} + f_{j,1} z^{-1} + \ldots. + f_{j,na} z^{-na}, \quad (8)$$
$$G_j\left(z^{-1}\right) = B\left(z^{-1}\right) E_j\left(z^{-1}\right), \quad (9)$$
$$A(z^{-1}) \xrightarrow{\text{singular}} \begin{cases} E_1 = 1 \\ F_1 = z(1 - \tilde{A}(z^{-1})) \end{cases} \to \begin{cases} E_{j+1}(z^{-1}) = E_j(z^{-1}) + f_{j,0} z^{-j} \\ f_{j+1,i} = f_{j,i+1} - f_{j,0}\tilde{a}_{i+1}, i = 0, \\ 1, \ldots, n_{\tilde{a}} - 1, \end{cases} \quad (10)$$

Equation (6) is a Diophantine equation, and $E_j\left(z^{-1}\right)$ and $F_j\left(z^{-1}\right)$ are Diophantine polynomials that are calculated by the recursive equation (10). For the predicted output (11):

$$\hat{y}\left(t+j\,|\,t\right) = G_j\left(z^{-1}\right) \Delta u\left(t+j-d+1\right) + F_j\left(z^{-1}\right) y\left(t\right), \quad (11)$$

$$Y = \underbrace{\phi Y_- + \pi U_-}_{\text{Free Response}} + \underbrace{\Omega U_+}_{\text{Force Response}}, \quad (12)$$
$$REF = [REF\,(t+d+1) \ldots\ldots .. REF\,(t+d+p)]^T,$$
$$J_c = (REF - Y)^T Q (REF - Y) + U_+^T R U_+ \to \frac{\partial J}{\partial U_+} = 0 \xrightarrow{\text{receding horizon}} \Delta u(t) = U_+(1,1),$$
$$\begin{cases} \Delta u_{\min} < \Delta u(t) < \Delta u_{\max} \\ u_{\min} < u(t) < u_{\max} \end{cases} \xrightarrow{\text{Constrains}} \begin{array}{l} -3 < \Delta T_{\text{ini,w}} < 3 \\ -20 < T_{\text{ini,w}} < 80 \end{array} \quad (13)$$

Y is the estimated model output of the vector along the prediction horizon. REF is the reference signal, and the R and Q matrices of the input and output weights are selected via repeated simulations as the results are continuously investigated. P is the prediction horizon, and M is the control horizon. $\Delta u\,(t)$ is the control signal variation obtained from (13). The $\Omega, \pi\phi$ matrices and U_+, U_-, Y_- are defined as follows:

$$\phi = \begin{bmatrix} f_{d+1,0} & \cdots & f_{d+1,na} \\ \vdots & \ddots & \vdots \\ f_{d+p,0} & \cdots & f_{d+p,na} \end{bmatrix}, Y_- = \begin{bmatrix} y\,(t) \\ \vdots \\ y\,(t-n_a) \end{bmatrix},$$
$$\pi = \begin{bmatrix} g_{d+1,1} & \cdots & g_{d+1,nb} \\ \vdots & \ddots & \vdots \\ g_{d+p,p} & \cdots & g_{d+p,nb} \end{bmatrix}, U_- = \begin{bmatrix} \Delta u\,(t-1) \\ \vdots \\ \Delta u\,(t-n_b) \end{bmatrix},$$
$$\Omega = \begin{bmatrix} g_{d+1,0} & \cdots & 0 \\ \vdots & \ddots & \vdots \\ g_{d+p,m-1} & \cdots & g_{d+p,0} \end{bmatrix}, U_+ = \begin{bmatrix} \Delta u\,(t) \\ \vdots \\ \Delta u\,(t+m-1) \end{bmatrix}, \quad (14)$$

The GPC controller is applied to the transfer function model, which is strictly proper and is estimated online each time the control algorithm is run using data from the outlet air temperature $T_{sa,i}$ and inlet water temperature $T_{ini,w}$; it should be noted that the latter datapoint is considered as a control variable. This model is updated during the execution of the control algorithm, and the effect of disturbances T_o, T_{ri} on the system's output is considered; there is therefore no need to enter them into the control algorithm. The computational burden is thus reduced. As the model is updated, **the adaptive constrained GPC controller** can adequately control the system perturbation by neutralizing disturbances and converging the output to the reference signal. $G_{e,i}$ is the transfer function that has been estimated online during the control for each AHU (Fig. 7). The degree of the transfer function is assumed to be equal to 3. This model has been estimated using the RLS algorithm [41]. $\theta(t)$ is the vector of the estimated parameters, which consist of the discrete transfer function parameters $G_{e,i}$. K(t) is the Kalman filter coefficient vector, P_e(t) is the covariance matrix, and $\varphi^1\,(t)$ is the regression matrix, which consists of measured output and control input signals. Finally, λ is the forgetting

factor:

$$\begin{aligned}\theta(t) &= \theta(t-1) + K(t)\left[y(t) - \varphi^T(t-1)\,\theta(t-1)\right],\\ K(t) &= P_e(t-1)\,\varphi^1(t-1)\\ &\quad \left[\lambda I + \varphi^T(t-1)\,P_e(t-1)\,\varphi(t-1)\right],\\ P_e(t) &= \frac{\left(I - K(t)\,\varphi^T(t-1)\right)P_e(t-1)}{\lambda}, \lambda = 1,\end{aligned} \tag{15}$$

$G_{e,i}$ is specified as follows:

$$\begin{aligned}&\textit{Estimated Transfer Function} \rightarrow\\ G_{e,i}(t) &= \frac{b_0(t)\,z^{-1} + b_1(t)\,z^{-2} + b_2(t)\,z^{-3}}{a_0 + a_1(t)\,z^{-1} + a_2(t)\,z^{-2} + a_3(t)\,z^{-3}}, a_0 = 1,\\ \theta(t) &= \left[a_1(t)\ a_2(t)\ a_3(t)\ b_0(t)\ b_1(t)\ b_2(t)\right]^T,\\ \varphi(t-1) &= \left[-T_{\mathrm{sa,i}}(t-1\cdots t-3)\ T_{\mathrm{ini,w}}(t-1\cdots t-3)\right]^T,\end{aligned} \tag{16}$$

In this section main goal is to control the output air temperature ($T_{sa,i}$) of each AHU. The proposed adaptive constrained generalized controller has been applied on estimated transfer function equation (16) that has been estimated online using dynamic recurrent neural network (that has been investigated in section II) control input variable (H/E inlet water $T_{ini,w}$) and model output ($T_{sa,i}$). The reference value for output ($T_{sa,ref}$) and recirculation air temperature (T_{ri}) have been considered using simulation dataset in [3]. Other variables used are from the real system dataset [4]. Outlet water temperature ($T_{outi,w}$) only is used to increase the accuracy of the overall model and close the estimated model to real system application. It also has been used in section IV for energy consumption calculation.

B. AHU OUTLET AIR HUMIDITY AND FLOW CONTROL, AND ENERGY CONSUMPTION OPTIMIZATION

The ventilation system's ability to maintain the humidity of the ventilated areas within the standard range is one of the essential points that should be considered because it is a crucial criterion for creating thermal comfort. The purpose is to keep the outlet airflow $G_{a,i}$ of each air conditioner constant and also to keep the relative humidity $H_{out,i}$ of the outlet air within the range specified by ASHRAE [42]. The humidity and output airflow rate has been controlled using the fan and a recirculation air damper system (Figure 3). An equation for the relative humidity percentage and airflow rate of the output air of each AHU is given below as per the instructions of [33]:

$$\begin{cases} G_{out,i} = G_o + G_{ri}\\ H_{out,i}G_{out,i} = H_{ri}G_{ri}OA_i + H_oG_o\\ H_{ri}(t) \in [25, 65]\\ G_{ri}(t) \in [0.6558, 0.8745],\\ G_0(t) \in [-0.0583, 0.0583]\,(\frac{kg}{s}), \end{cases} \tag{17}$$

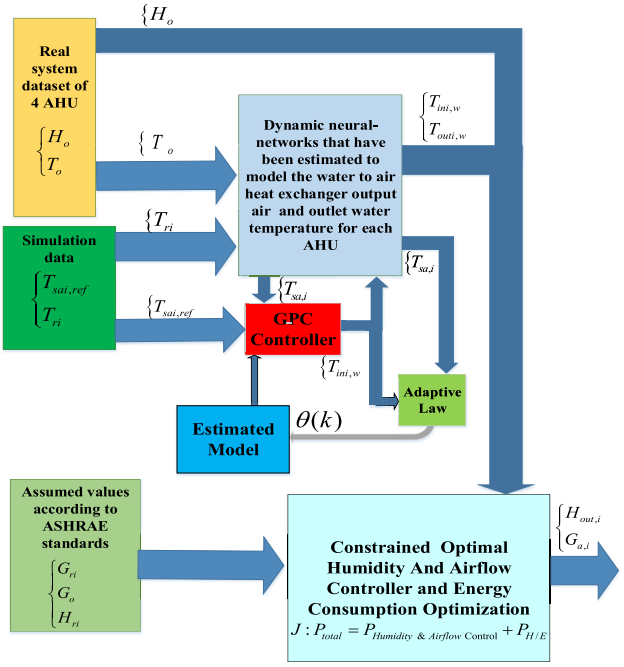

FIGURE 7. Block diagram of the control system for each AHU unit.

In this section, according to the real system dataset and (17), just H_o is known. The values of the other variables are unknown. To demonstrate the optimal constrained controller's ability to control the system, the values of the unknown variables G_o, G_{ri} have been chosen to be within the range that will ensure that the assumed value for every AHU capacity and its outlet airflow ($1700m^3.h, 0.583kg.s^{-1}$) track the reference with accuracy [3]. These variables are random values in specific ranges. H_{ri} is also a random value, and its range has been chosen according to ASHRAE standards. The main goal of this work is to reduce the energy consumption of each AHU over the period of one year. In the constrained optimal controller implemented in this section, the cost function contemplates the total power of the H/E as well as the fan and damper system. Humidity and exhaust airflow are controlled so that, in addition to maintaining their value within the specified range, the power consumption of the system is also minimized. According to "Fan laws" in [34], [43], the overall form of the fan power can be specified in the HVAC design with this equation:

$$\begin{cases} P_0 = 0.1\,(kW)\,, G_{out,i} \overset{ControlGoal}{\longrightarrow}\\ G_{a,i} = 0.583\ kg.s^{-1},\\ P_{Humidity\ \&\ Airflow\ Control}\\ = P_0 \dfrac{(G_{a,i}=0.583)^6}{(G_{out,i}=\dfrac{H_{ri}G_{ri}OA_i + H_oG_o}{H_{out,i}})^6}, (kW) \end{cases} \tag{18}$$

For the H/E, the power consumption can be expressed as:

$$P_{H/E} = \frac{G_w c_w}{T_s}\left|(T_{ini.w} - T_{outi,w})\right|\,(kW) \tag{19}$$

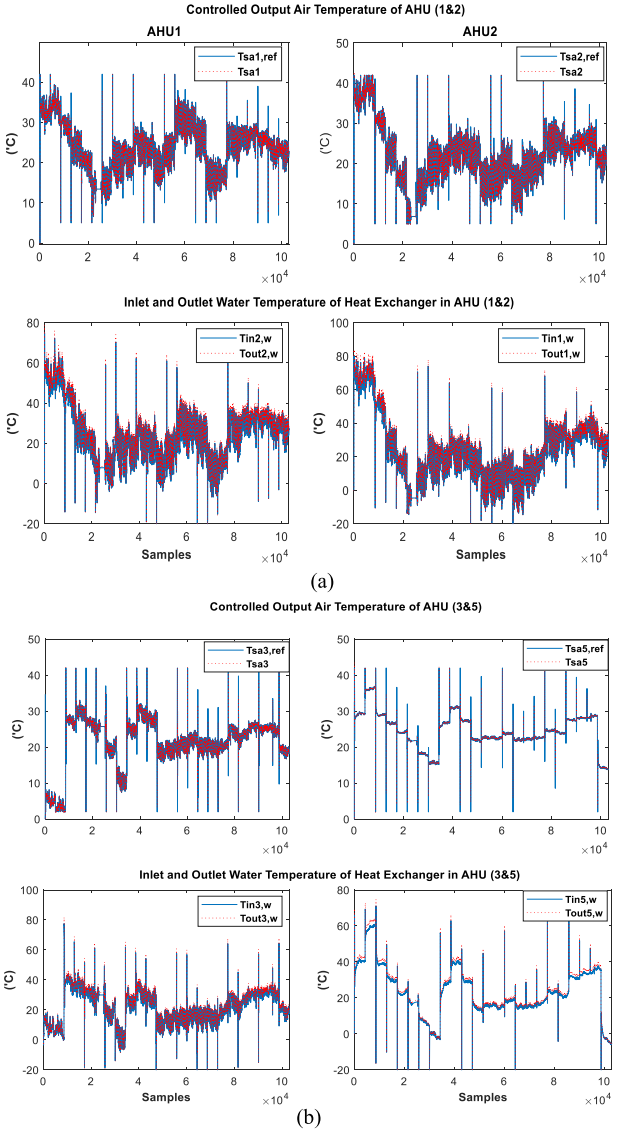

FIGURE 8. **(a) (b) Outlet temperature controller simulation results for $AHU_{1,2}$ & $AHU_{3,5}$.**

The optimal constrained controller (Fig. 7) cost function J and constraints are:

$$\begin{cases} J\ (OA_i) : P_{total} = P_{Humidity\ \&\ Airflow\ Control} + P_{\mathrm{H/E}} \\ 30 \leq H_{out,i} \leq 60. (20) \\ 0.965 G_{a,i} \leq G_{out,i} \leq G_{a,i},\ 0.2 \leq \mathrm{OA}_i \\ \leq 1\ (\text{Damper Opening Percentage})\ . \end{cases} \tag{20}$$

This controller has been simulated in MATLAB, and the ''fmincon'' algorithm has been used for optimization. The results are shown in Fig. 10.

IV. DISCUSSION OF CONTROLLER SIMULATION RESULTS

In section 3.1, the adaptive constrained GPC has been applied to each AHU. The controller parameters (P, M, and the degree of Ge in the transfer function) play an essential role in the volume of the controller calculations. In this work,

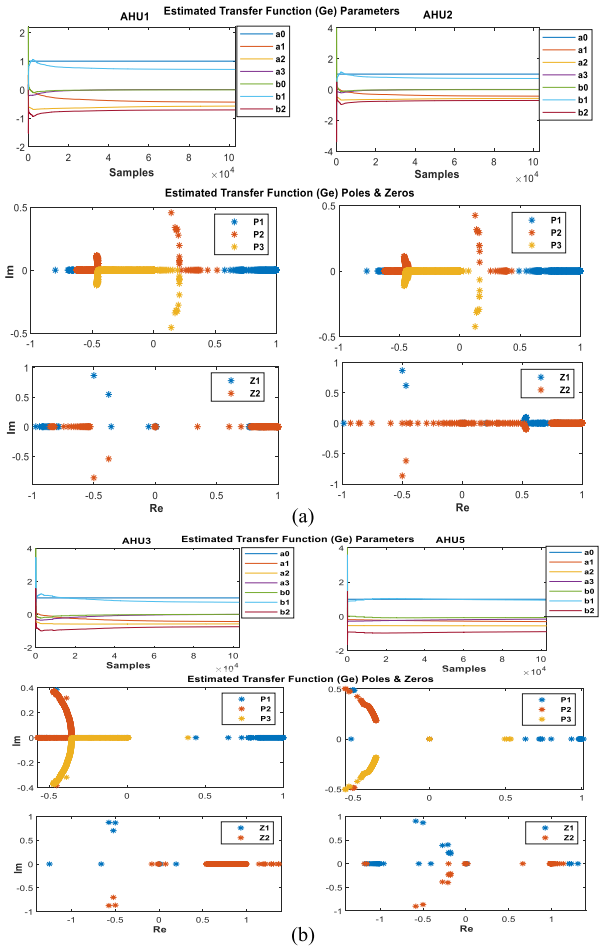

FIGURE 9. **(a) (b) Estimated model $G_{e,i}$ parameters, closed-loop poles, and zeros during the control algorithm of $AHU_{1,2}$& $AHU_{3,5}$.**

these parameters are selected such that the computational load and dimensions of the controller matrices (ϕ, π, Ω) are minimized. In contrast, the controller can properly manage the outlet air temperature of each AHU. These parameters, the weight matrices Q and U, and the constraint related to the changes of the control signal ($\Delta T_{ini.w}$) are determined by repeating the system simulation over a period of one year and reviewing the results to obtain a favorable response are shown in Fig 8. The control signal constraint ($T_{ini.w}$) is also determined by the results of section 2. Figure 2 shows that the outlet air temperature ($T_{\mathrm{sa,i}}$) of each AHU is well converged to the reference signal ($T_{\mathrm{sai,ref}}$). The temperature of the inlet and outlet water of the H/E($T_{ini.w}$, $T_{outi,w}$) have also been determined. Figure 3 shows that the parameters of the conversion function that are estimated online converge rapidly to a constant value when the control algorithm is executed. The poles of the model are also located within the unit circle, indicating that the closed-loop system is stable (Fig 9). In section 3.2, the constrained optimal controller is implemented on the system to control the relative humidity and airflow of each AHU; the minimization of the energy used by each air conditioner is also considered.

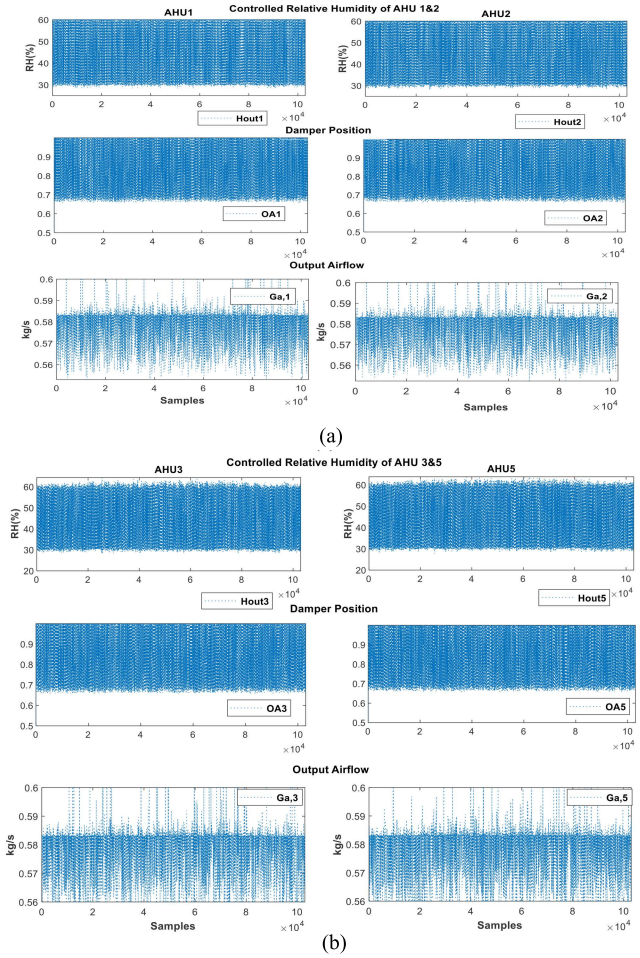

FIGURE 10. (a) (b) Constrained optimal controller simulation results.

The power consumption of the H/E is calculated using the difference between its inlet and outlet water temperatures, which is added to the power consumption of the airflow and humidity control system eq(20). The dataset used in this system is that of a ventilation system in a country with four distinct seasons that range from hot to cold, which further emphasizes the importance of optimizing the ventilation system's energy consumption. This simulation was performed over a period of one year with a sampling time of 300 seconds, which was chosen based on the real system dataset in [4]. The energy consumption of the air conditioning system was calculated and compared with the energy consumption published in [3], which was calculated using the overall energy consumption equation; the two studies were performed in similar conditions. The results are given in Table 1. The simulation results show a return of more than 54%.

This study is based on a simulation. It is important to explain how to implement this control system on the real system. The implementation can be done in two ways: adaptive and non-adaptive. In the non-adaptive mode, data related to the closed-loop system of the ventilated areas are collected. In the next step, the reference signal temperature

TABLE 1. Energy consumption of AHUs during one year (kW.h).

AHU	Dataset on-off controller[4]	PI controller on one year model[3]	DMPC in one year (SSNN) model [3]	Energy consumption using proposed controllers for 4 AHU units*
AHU1	2420.7	1655.6	1840.8	703.90(61.7%), (70.9%) ↓
AHU2	2781.2	1590.9	1659.0	657.36(60.3%), (73.6%) ↓
AHU3	1957.2	1731.6	1623.0	724.45(55.3%), (62.9%) ↓
AHU5	2254.0	1633.3	1147.0	738.79(35.6%), (67.2%) ↓
Total	9413.1	6611.4	6269.8	2824.5(54.9%), (69.9%) ↓

of the AHU outlet is determined. After collecting this data, the inlet and outlet water temperatures are estimated by measuring the actual parameters of the H/E. In the temperature control section, the model of the dynamic neural networks is estimated using the data collected from the system. In this case, this neural network acts as the controller. Then, the only computational load is in the section that controls the humidity and exhaust airflow. In the non-adaptive mode, if the system's operating conditions change, the model needs to be re-estimated. In the adaptive mode, the system is more resilient to real system disturbances because the transfer function model used in the temperature controller is estimated online based on the inlet water temperature and the outlet air temperature. This method has a higher computational load, but it provides better system stability.

Efforts have also been made to minimize the computational burden. One of the disadvantages of MPC is its computational load, which necessitates robust hardware. Arduino-based boards can be used to control each AHU by sending commands and collecting the data of the measured variables. For larger buildings, PLC-based hardware can be used. It is also possible to implement the proposed control algorithm on a central PC using MATLAB software and its Arduino toolbox. This study uses a Windows laptop with Intel Corei7-4702MQ CPU, 12 GB of ram, and the MATLAB and Simulink software. The total simulation time with a sampling time of 300 seconds and 102,980 total samples was about six hours, or about 0.21 seconds for each sequence in the adaptive mode.

V. CONCLUSION

Optimizing the energy consumption of ventilation systems is one of the most important challenges that should always be considered in smart buildings. In this article, in addition to keeping the temperature and humidity of the ventilation system's AHUs within the desired thermal comfort range, we also attempt to minimize each AHU's energy usage by investigating the consumption of their components. The dynamic neural network model of the water-to-air H/E is estimated using real data, data obtained from the simulation of a ventilation system with four AHUs, and the proposed dynamic model of the water-to-air H/E. The adaptive constrained generalized predictive controller has also been implemented on the H/E model to improve the system output's convergence to the reference value as well as the system's response to disturbances and possible changes in its parameters; the stability of the system is thus

bolstered. In the design of this controller, an attempt has been made to minimize the computational load by simplifying the model on which it is implemented. The results show that the AHUs' energy consumption is reduced by more than 54%.

REFERENCES

[1] B. Dean, J. Dulac, K. Petrichenko, and P. Graham, "Towards zero-emission efficient and resilient buildings: Global Status Report," Global Alliance Buildings Construct. (GABC), 2016. [Online]. Available: https://orbit.dtu.dk/en/publications/towards-zero-emission-efficient-and-resilient-buildings-global-st

[2] M. Razmara, M. Maasoumy, M. Shahbakhti, and R. D. Robinett, III, "Optimal exergy control of building HVAC system," *Appl. Energy*, vol. 156, pp. 555–565, Oct. 2015.

[3] O. Asvadi-Kermani and H. Momeni, "A constrained distributed time-series neural network MPC approach for HVAC system energy saving in a medium-large building," *J. Building Perform. Simul.*, vol. 14, no. 4, pp. 383–400, Jul. 2021.

[4] G. Stamatescu. *HVAC Air Handling Units: One-Year Data From Medium-to-Large Size Academic Building*. Accessed: Mar. 15, 2019. [Online]. Available: https://ieee-dataport.org/documents/hvac-air-handling-units-one-year-data-medium-large-size-academic-building

[5] G. T. Costanzo, S. Iacovella, F. Ruelens, T. Leurs, and B. J. Claessens, "Experimental analysis of data-driven control for a building heating system," *Sustain. Energy, Grids Netw.*, vol. 6, pp. 81–90, Jun. 2016.

[6] S. Yang, M. P. Wan, W. Chen, B. F. Ng, and S. Dubey, "Experiment study of machine-learning-based approximate model predictive control for energy-efficient building control," *Appl. Energy*, vol. 288, Apr. 2021, Art. no. 116648.

[7] R. Ž. Jovanović, A. A. Sretenović, and B. D. Živković, "Ensemble of various neural networks for prediction of heating energy consumption," *Energy Buildings*, vol. 94, pp. 189–199, May 2015.

[8] A. Afram, F. Janabi-Sharifi, A. S. Fung, and K. Raahemifar, "Artificial neural network (ANN) based model predictive control (MPC) and optimization of HVAC systems: A state of the art review and case study of a residential HVAC system," *Energy Buildings*, vol. 141, pp. 96–113. Apr. 2017.

[9] M. Killian and M. Kozek, "Ten questions concerning model predictive control for energy efficient buildings," *Building Environ.*, vol. 105, pp. 403–412, Aug. 2016.

[10] S. Prívara, J. Cigler, Z. Vána, F. Oldewurtel, C. Sagerschnig, and E. Žáceková, "Building modeling as a crucial part for building predictive control," *Energy Buildings*, vol. 56, pp. 8–22, Jan. 2013.

[11] H. Fontenot and B. Dong, "Modeling and control of building-integrated microgrids for optimal energy management—A review," *Appl. Energy*, vol. 254, Nov. 2019, Art. no. 113689.

[12] S. Yang, M. P. Wan, B. F. Ng, S. Dubey, G. P. Henze, W. Chen, and K. Baskaran, "Experimental study of model predictive control for an air-conditioning system with dedicated outdoor air system," *Appl. Energy*, vol. 257, Jan. 2020, Art. no. 113920.

[13] U. Amin, M. J. Hossain, and E. Fernandez, "Optimal price based control of HVAC systems in multizone office buildings for demand response," *J. Cleaner Prod.*, vol. 270, Oct. 2020, Art. no. 122059.

[14] R. Z. Homod, K. S. Gaeid, S. M. Dawood, A. Hatami, and K. S. Sahari, "Evaluation of energy-saving potential for optimal time response of HVAC control system in smart buildings," *Appl. Energy*, vol. 271, Aug. 2020, Art. no. 115255.

[15] J. Cígler, D. Gyalistras, J. Široky, V. Tiet, and L. Ferkl, "Beyond theory: The challenge of implementing model predictive control in buildings," in *Proc. 11th Rehva World Congr. (Clima)*, vol. 250, Jun. 2013.

[16] P. Rockett and E. A. Hathway, "Model-predictive control for non-domestic buildings: A critical review and prospects," *Building Res. Inf.*, vol. 45, no. 5, pp. 556–571, 2017.

[17] Y. Chen, Z. Tong, Y. Zheng, H. Samuelson, and L. Norford, "Transfer learning with deep neural networks for model predictive control of HVAC and natural ventilation in smart buildings," *J. Cleaner Prod.*, vol. 254, May 2020, Art. no. 119866.

[18] F. Behrooz, N. Mariun, M. H. Marhaban, M. A. M. Radzi, and A. R. Ramli, "Review of control techniques for HVAC systems-nonlinearity approaches based on fuzzy cognitive maps," *Energies*, vol. 11, no. 3, p. 495, 2018.

[19] X. Li and J. Wen, "Review of building energy modeling for control and operation," *Renew. Sustain. Energy Rev.*, vol. 37, pp. 517–537, Sep. 2014.

[20] A. Afram and F. Janabi-Sharifi, "Theory and applications of HVAC control systems—A review of model predictive control (MPC)," *Building Environ.*, vol. 72, pp. 343–355, Feb. 2014.

[21] E. Á. R. Jara, F. J. S. de la Flor, S. Á. Domínguez, J. L. M. Félix, and J. M. S. Lissén, "A new analytical approach for simplified thermal modelling of buildings: Self-adjusting RC-network model," *Energy Buildings*, vol. 130, pp. 85–97, Oct. 2016.

[22] K. Le, R. Bourdais, and H. Guéguen, "From hybrid model predictive control to logical control for shading system: A support vector machine approach," *Energy Buildings*, vol. 84, pp. 352–359, Dec. 2014.

[23] G. Lymperopoulos and P. Ioannou, "Building temperature regulation in a multi-zone HVAC system using distributed adaptive control," *Energy Buildings*, vol. 215, May 2020, Art. no. 109825.

[24] Y. Li and Z. Tong, "Model predictive control strategy using encoder-decoder recurrent neural networks for smart control of thermal environment," *J. Building Eng.*, vol. 42, Oct. 2021, Art. no. 103017.

[25] W. Liu, R. Kalbasi, and M. Afrand, "Solutions for enhancement of energy and exergy efficiencies in air handling units," *J. Cleaner Prod.*, vol. 257, Jun. 2020, Art. no. 120565.

[26] J. M. Lee, S. H. Hong, B. M. Seo, and K. H. Lee, "Application of artificial neural networks for optimized AHU discharge air temperature set-point and minimized cooling energy in VAV system," *Appl. Thermal Eng.*, vol. 153, pp. 726–738, May 2019.

[27] A. Kusiak, Y. Zeng, and G. Xu, "Minimizing energy consumption of an air handling unit with a computational intelligence approach," *Energy Buildings*, vol. 60, pp. 355–363, May 2013.

[28] S. Sayadi, G. Tsatsaronis, T. Morosuk, M. Baranski, R. Sangi, and D. Müller, "Exergy-based control strategies for the efficient operation of building energy systems," *J. Cleaner Prod.*, vol. 241, Dec. 2019, Art. no. 118277.

[29] Y. Chen and S. Treado, "Development of a simulation platform based on dynamic models for HVAC control analysis," *Energy Buildings*, vol. 68, pp. 376–386, Jan. 2014.

[30] Z. Liu, W. Li, Y. Chen, Y. Luo, and L. Zhang, "Review of energy conservation technologies for fresh air supply in zero energy buildings," *Appl. Thermal Eng.*, vol. 148, pp. 544–556, Feb. 2019.

[31] J.-H. Chen, H.-T. Yau, and T.-H. Hung, "Design and implementation of FPGA-based Taguchi-chaos-PSO sun tracking systems," *Mechatronics*, vol. 25, pp. 55–64, Feb. 2015.

[32] C.-L. Chen, C.-E. Ho, and H.-T. Yau, "Performance analysis and optimization of a solar powered stirling engine with heat transfer considerations," *Energies*, vol. 5, no. 9, pp. 3573–3585, Sep. 2012.

[33] Y. Yao and Y. Yu, *Modeling and Control in Air-Conditioning Systems*. Berlin, Germany: Springer-Verlag GmbH, 2017.

[34] A. H. Ashrae, *HVAC Systems and Equipment*. Atlanta, GA, USA: American Society of Heating, Refrigerating, and Air-Conditioning Engineers, 2008.

[35] T. Lubbers. 15 × 15 *Water to Air Heat Exchanger 1″ Copper Ports*. [Online]. Available: https://www.thelogboiler.com/product/15x15-water-to-air-heat-exchanger-1-copper-ports-with-install-kit/

[36] L. G. B. Ruiz, M. P. Cuéllar, M. D. Calvo-Flores, and M. D. C. P. Jiménez, "An application of non-linear autoregressive neural networks to predict energy consumption in public buildings," *Energies*, vol. 9, no. 9, p. 684, 2016.

[37] M. Beale, M. Hagan, and H. Demuth. (2020). *Pdf Documentation: MATLAB Deep Learning Toolbox User's Guide*. [Online]. Available: https://uk.mathworks.com/help/deeplearning.

[38] M. Hagan and M. Menhaj, "Improvement of the neighborhood based Levenberg–Marquardt algorithm by local adaptation of the learning coefficient," *IEEE Trans. Neural Netw.*, vol. 5, no. 6, pp. 989–993, Jul. 1994.

[39] E. F. Camacho and C. B. Alba, *Model Predictive Control*. London, U.K.: Springer-Verlag, 2013.

[40] O. Asvadi-Kermani, B. Felegari, and H. Momeni, "Adaptive constrained generalized predictive controller for the PMSM speed servo system to reduce the effect of different load torques," *e-Prime, Adv. Electr. Eng., Electron. Energy*, vol. 2, Jan. 2022, Art. no. 100032.

[41] K. J. Åström and B. Wittenmark, *Adaptive Control*. Chelmsford, MA, USA: Courier Corporation, 2013.

[42] *ASHRAE Handbook—-Fundamentals*, 2nd ed., Amer. Soc. Heating, Refrigerating Air-Conditioning Eng., Atlanta, GA, USA, 2009.

[43] Captiveaire. *Designing Air Flow Systems*. Accessed: Jan. 1, 2021. [Online]. Available: https://www.captiveaire.com/manuals/airsystemdesign/designairsystems.htm

OMID ASVADI-KERMANI (Graduate Student Member, IEEE) received the B.Sc. degree in control engineering from Tabriz University, in 2018, and the M.Sc. degree in control systems engineering from Tarbiat Modares University, in 2021. His research interests include building energy systems, heating and ventilation air conditioning systems, electrical drives, and industrial electronics.

HAMIDREZA MOMENI (Senior Member, IEEE) was born in Khomain, Iran, in 1954. He received the B.Sc. degree in electrical engineering from the Sharif University of Technology, in 1977, the M.Sc. degree in electrical engineering from the University of Wisconsin–Madison, Madison, WI, USA, in 1979, and the Ph.D. degree in electrical engineering from Imperial College London, U.K., in 1987. He is currently a Professor with the Electrical Engineering Department, University of Tarbiat Modarres, Tehran, Iran. His research interests include adaptive control, robust control, fractional systems, teleoperation systems, industrial control, instrumentation, automation, and navigation and guidance.

ANDREA JUSTO received the B.Sc. and M.Sc. degrees in electrical engineering from the School of Mechanical and Electrical Engineering Zacatenco Area: Electrical Power Systems, National Polytechnic Institute (IPN), Mexico, in 2018 and 2021, respectively. She is currently pursuing the M.Sc. degree in psychobiology and cognitive neuroscience with the Autonomous University of Barcelona. Her research interests include microgrids, biological ecosystems, and cognitive neuroscience.

JOSEP M. GUERRERO (Fellow, IEEE) received the B.S. degree in telecommunications engineering, the M.S. degree in electronics engineering, and the Ph.D. degree in power electronics from the Technical University of Catalonia, Barcelona, in 1997, 2000, and 2003, respectively. Since 2011, he has been a Full Professor with the Department of Energy Technology, Aalborg University, Denmark, where he is responsible for the Microgrid Research Program. He has been the Chair Professor with Shandong University, since 2014, a Distinguished Guest Professor with Hunan University, since 2015, a Visiting Professor Fellow with Aston University, U.K., since 2016, and a Guest Professor with the Nanjing University of Posts and Telecommunications. In 2019, he became a Villum Investigator. He has published more than 500 journal articles in the fields of microgrids and renewable energy systems, which are cited more than 30,000 times. His research interests include oriented to different microgrid aspects, including power electronics, distributed energy storage systems, hierarchical and cooperative control, energy management systems, smart metering, and the Internet of Things for ac/dc microgrid clusters and islanded minigrids, recently specially focused on maritime microgrids for electrical ships, vessels, ferries, and seaports. In 2015, he was elevated as a fellow of IEEE for his contributions on "Distributed Power Systems and Microgrids." He received the Best Paper Award of the IEEE TRANSACTIONS ON ENERGY CONVERSION from 2014 to 2015, the Best Paper Prize of IEEE-PES in 2015, and the Best Paper Award of the *Journal of Power Electronics* in 2016. For five consecutive years, from 2014 to 2018, he was awarded by Clarivate Analytics (former Thomson Reuters) as the Highly Cited Researcher. He is an associate editor for a number of IEEE TRANSACTIONS.

JUAN C. VASQUEZ (Senior Member, IEEE) received the Ph.D. degree in automatic control, robotics, and computer vision from the Barcelona Tech—UPC, Spain, in 2009. In 2019, he became a Full Professor with the Department of Energy Technology, Aalborg University, Denmark, where he is currently the Vice Director of the Center for Research on Microgrids (crom.et.aau.dk). He was a Visiting Scholar with the Center of Power Electronics Systems (CPES), Virginia Tech; and a Visiting Professor with Ritsumeikan University, Japan. He has published more than 500 journal articles in the field of microgrids, which are cited more than 25,000 times. His current research interests include operation, advanced hierarchical and cooperative control, optimization, and energy management applied to distributed generation in ac/dc microgrids, maritime microgrids, advanced metering infrastructures, and the integration of the Internet of Things and energy internet into the smartgrid. Since 2017, he has been awarded by the Thomson Reuters as a Highly Cited Researcher. He was a recipient of the Young Investigator Award in 2019. He is an Associate Editor of *IET Power Electronics* and the IEEE SYSTEMS JOURNAL and a Guest Editor of a Special Issue on the IEEE TRANSACTIONS ON INDUSTRIAL INFORMATICS on "Energy Internet."

JOSE RODRIGUEZ (Life Fellow, IEEE) received the Engineering degree in electrical engineering from the Universidad Tecnica Federico Santa Maria, Valparaiso, Chile, in 1977, and the Dr.-Ing. degree in electrical engineering from the University of Erlangen, Erlangen, Germany, in 1985. He has been with the Department of Electronics Engineering, Universidad Tecnica Federico Santa Maria, since 1977, where he was a Full Professor and the President. From 2015 to 2019, he was the President of Universidad Andres Bello, Santiago, Chile. Since 2022, he has been the President of Universidad San Sebastian, Santiago. He has coauthored two books, several book chapters, and more than 700 journal and conference papers. His main research interests include multilevel inverters, new converter topologies, control of power converters, and adjustable-speed drives. He is a member of the Chilean Academy of Engineering. He has received a number of best paper awards from journals of the IEEE. In 2014, he received the National Award of Applied Sciences and Technology from the Government of Chile. In 2015, he received the Eugene Mittelmann Award from the Industrial Electronics Society of the IEEE. From 2014 to 2020, he has been included in the list of Highly Cited Researchers published by Web of Science.

BASEEM KHAN (Senior Member, IEEE) received the B.Eng. degree in electrical engineering from Rajiv Gandhi Technological University, Bhopal, India, in 2008, and the M.Tech. and D.Phil. degrees in electrical engineering from the Maulana Azad National Institute of Technology, Bhopal, in 2010 and 2014, respectively. He is currently working as a Faculty Member at Hawassa University, Ethiopia. He has published more than 125 research articles in indexed journals, including IEEE TRANSACTIONS, IEEE ACCESS, *Computer and Electrical Engineering* (Elsevier), *IET GTD*, *IET PRG*, and *IET Power Electronics*. Further, he has authored and edited books with Wiley, CRC Press, and Elsevier. His research interests include power system restructuring, power system planning, smart grid technologies, meta-heuristic optimization techniques, reliability analysis of renewable energy systems, power quality analysis, and renewable energy integration.